

# Journal of Materials Chemistry C

Accepted Manuscript



This article can be cited before page numbers have been issued, to do this please use: L. Wang, Y. Li, X. You, K. Xu, Q. Feng, J. Wang, Y. Liu, K. Li and H. Hou, *J. Mater. Chem. C*, 2016, DOI: 10.1039/C6TC03791G.



This is an Accepted Manuscript, which has been through the Royal Society of Chemistry peer review process and has been accepted for publication.

Accepted Manuscripts are published online shortly after acceptance, before technical editing, formatting and proof reading. Using this free service, authors can make their results available to the community, in citable form, before we publish the edited article. We will replace this Accepted Manuscript with the edited and formatted Advance Article as soon as it is available.

You can find more information about Accepted Manuscripts in the [author guidelines](#).

Please note that technical editing may introduce minor changes to the text and/or graphics, which may alter content. The journal's standard [Terms & Conditions](#) and the ethical guidelines, outlined in our [author and reviewer resource centre](#), still apply. In no event shall the Royal Society of Chemistry be held responsible for any errors or omissions in this Accepted Manuscript or any consequences arising from the use of any information it contains.



## Journal Name

## ARTICLE

## Erasable Photo-patterning Material Based on a Specially Designed 4-(1,2,2-triphenylvinyl)aniline Salicylaldehyde Hydrazone Aggregation-Induced Emission (AIE) Molecule

Received 00th January 20xx,  
Accepted 00th January 20xx

DOI: 10.1039/x0xx00000x

www.rsc.org/

Lili Wang,<sup>a</sup> Yuanyuan Li,<sup>b</sup> Xuejiao You,<sup>a</sup> Kui Xu,<sup>a</sup> Qi Feng,<sup>a</sup> Jinmin Wang,<sup>a</sup> Yuanyuan Liu,<sup>a</sup> Kai Li,<sup>\*a</sup> and Hongwei Hou<sup>\*a</sup>

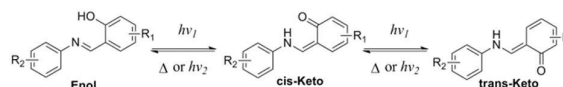
Luminescent molecules with photochromic properties show strong potential in molecular switches, molecular logic gates, photo-controllable materials, bio-imaging, anti-counterfeiting, photo-patterning, etc. However, there is still rare of research in such molecule exhibiting reversible photo-controllable color and fluorescence change in solid states, which due to the aggregation-caused quenching (ACQ) effect of most luminogens. In this work, a reversible photochromic molecule (**1**) with aggregation-induced emission (AIE) property was developed. Compound **1** exhibits typical AIE properties as a result of restricted intramolecular rotations (RIR) and excited-state intramolecular proton transfer (ESIPT) processes. As a photochromic molecule, compound **1** shows reversible color and fluorescence changes upon UV light irradiation with good fatigue resistance. More importantly, conversion rate from its irradiated form to initial form is controllable by temperature and long wavelength light irradiation, which make it suitable for photo-patterning material with erasable property.

### 1 Introduction

Luminescent materials have attracted much attention due to their diverse applications in chemistry, physics, material science, and biology.<sup>1</sup> However, most of their practical uses are usually limited by the notorious aggregation-caused quenching (ACQ) phenomenon: luminogens exhibit good fluorescence in dilute solutions but weak or even no fluorescence in concentrated solution or solid state as a result of the self-quenching effect of adjacent molecules.<sup>2</sup> In 2001, a novel luminescence phenomenon of aggregation-induced emission (AIE) was first observed by the group of Tang, which is exactly opposite to the ACQ effect: the emission of luminogens were very weak in solution but became intense when aggregates formed.<sup>3</sup> Since then, a variety of AIE systems (tetraphenylethenes (TPE), hexaphenylsilole (HPS), cyanostilbenes and salicylaldehyde (SA), etc.) were reported in succession, which have been widely applied in the field of organic light-emitting diodes (OLEDs), chemical sensors and multifunctional luminescent material.<sup>4</sup>

Recently, Tang and co-workers have successfully expand the application of AIE luminogens by developing a photo-activatable AIE system based on a caged TPE derivative.<sup>5</sup> The

fluorescence emission of the AIE group was partially or completely quenched by the quencher but can be recovered upon cleavage of the quencher under UV stimuli. A following work of another photo-activatable AIE system based on caged SA derivatives were reported by Xiang and Tong's group.<sup>6</sup> These novel photochromic systems show great potential of application in photo-patterning, photo-activatable imaging and anti-counterfeiting related areas. However, the photochromism of these caged fluorophores are irreversible, which limit their applications.<sup>7</sup> To overcome this challenge, some new strategies in the design of irreversible photo-controllable AIE system have been introduced such as photo-induced redox reactions and photo-induced cyclization reactions. Nevertheless, the fatigue resistances of these photochromic systems are still unsatisfactory.<sup>8</sup>



**Scheme 1.** Photochromic mechanism of salicylaldehyde hydrazone upon UV irradiation.

According to the reports, salicylaldehyde hydrazone is a reversible photochromic group with good fatigue resistance.<sup>9</sup> Upon UV irradiation, there is a reversible tautomerism between its enol-form and keto-forms (Scheme 1). Notably, the enol-form of salicylaldehyde hydrazone is beneficial for fluorescence emission due to an excited-state intramolecular proton transfer (ESIPT) process.<sup>10</sup> The keto-forms of salicylaldehyde hydrazone, in contrast, is a typical fluorescence quenching unit due to its strong electron-withdrawing

<sup>a</sup> College of Chemistry and Molecular Engineering, Zhengzhou University, Henan 450001, P. R. China. \*E-mail: likai@zzu.edu.cn or houghongw@zzu.edu.cn.

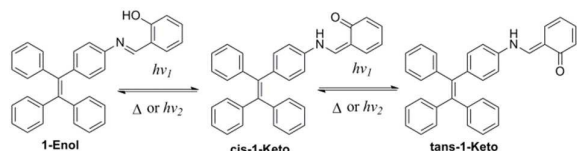
<sup>b</sup> School of Chemistry and Chemical Engineering, Henan University of Technology, Henan 450001, P. R. China.

Electronic Supplementary Information (ESI) available: Selected spectra and data referred in the paper; detailed crystal data and structure refinement for **1**. CCDC reference number 1472291. For ESI and crystallographic data in CIF or other electronic format see: 10.1039/x0xx00000x

## ARTICLE

## Journal Name

property.<sup>11</sup> These unique properties of salicylaldehyde hydrazone suggest that it could be used as a photo-controllable quencher in the design of photo-controllable luminescent molecules.



**Scheme 2.** Proposed mechanism for the color change of **1** upon UV irradiation.

In this work, a reversible photochromic AIE molecule was developed by connecting salicylaldehyde hydrazone with a typical AIE moiety of TPE (Scheme 2). This specially designed AIE molecule of 4-(1,2,2-triphenylvinyl)aniline salicylaldehyde hydrazone (**1**) exhibited reversible photochromic property with significant fluorescence change. Before UV irradiation, **1** was yellow and exhibited strong fluorescence emission in aggregative state. After UV irradiation, **1** turned to red and the fluorescence emission declined significantly. The good fatigue resistance property of **1** enables it to be applied in reversible photo-patterning and anti-counterfeiting related applications.

## 2 Experimental

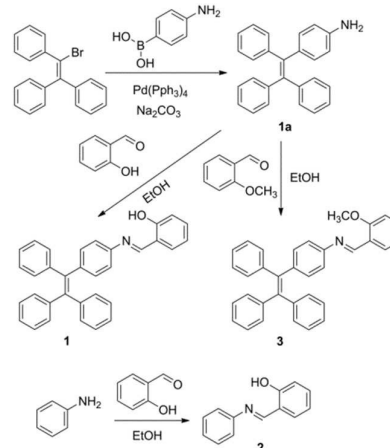
### 2.1. Materials.

Salicylaldehyde, aniline, (2-bromoethene-1,1,2-triyl)tribenzene, 4-aminobenzeneboronic acid hydrochloride, o-anisaldehyde, tetrabutylammonium bromide (TBAB) were purchased from J&K Chemical Co., Beijing, China. All the other materials were purchased from Sinopharm Chemical Reagent Beijing Co., Beijing, China. In these experiments, all the materials of analytical grade were used without further purification.

### 2.2. Characterizations.

<sup>1</sup>H and <sup>13</sup>C NMR spectra were recorded on a Bruker 400 Avance NMR spectrometer operated at 400 MHz. UV-Vis absorption spectra were recorded on a JASCO V-750 spectrophotometer. UV-Vis diffuse reflectance spectra were measured by Agilent Cary 5000 UV-Vis-NIR Spectrometer, BaSO<sub>4</sub> was used as reference. Fluorescence spectra were obtained on a Hitachi F-4600 spectrometer. Fluorescence lifetimes and quantum yields were recorded on Edinburgh FIS-980 fluorescence spectrometer. Dynamic light scattering (DLS) experiments were performed by a NanoPlus-3 dynamic light scattering particle size/zeta potential analyzer at room temperature. ESI-MS spectra were obtained on Agilent Technologies 6420 triple quadrupole LC/MS without using the LC part. Elemental analysis experiments were carried out on a Flash EA 1112 automatic element analyzer. Single-crystal X-ray diffraction intensity data were collected on a Rigaku Saturn 724 CCD diffractometer with Mo K $\alpha$  radiation ( $\lambda = 0.71073$  Å) at room temperature. X-ray Powder Diffraction (XRD) patterns were obtained by a PANalytical X'Pert PRO diffractometer. The

photos and videos were carried with Nikon D5500 camera. Laser of 405 nm used in Video 1 was produced by LD-T405F00 laser pointer (power output 20 mW). Visible light used in Video 1 and light sources used in Table S1 and Figure 10 were produced by a CEL-HXF300/CEL-HXUV300 xenon light source with different optical filters.



**Scheme 3.** Synthetic routes for compound **1**, **2** and **3**.

### 2.3. Synthesis.

Compounds **1-3** were synthesized according to the synthetic routes shown in Scheme 3. The new compounds were characterized by NMR spectra and ESI-MS spectra. Detailed synthetic procedures and characterization data are shown below and in Supplementary Information.

**4-(1,2,2-triphenylvinyl)aniline salicylaldehyde hydrazone (1).** 4-(1,2,2-triphenylvinyl)aniline (**1a**) was prepared through a reported procedure.<sup>12</sup> Salicylaldehyde (0.73 g, 6 mmol) and compound **1a** (1.73 g, 5 mmol) was dissolved in 30 mL absolute ethanol in a 50 mL flask. The stirred mixture was heated to 90 °C for 2 h. Then the solvent was concentrated to 10 mL under reduced pressure and cooled to 4 °C. After that, **1** (2.08 g, 4.6 mmol) was obtained as a yellow precipitate with a yield of 92%. <sup>1</sup>H NMR (400 MHz, CDCl<sub>3</sub>),  $\delta$  (ppm): 6.90 (m, 1H), 7.07 (m, 20H), 7.35 (m, 2H), 8.58 (s, 1H). <sup>13</sup>C NMR (400 MHz, CDCl<sub>3</sub>),  $\delta$  (ppm): 117.34, 119.31, 120.50, 127.70, 131.34, 131.37, 131.40, 140.14, 141.50, 142.90, 143.54, 143.59, 143.63, 161.92. ESI-MS spectrometry:  $m/z$  calcd. for [M+H]<sup>+</sup>: 452.2; found: 452.2. Elemental analysis, calcd. For C<sub>33</sub>H<sub>25</sub>NO: C, 87.77; H, 5.58; N, 3.10, found: C, 88.24; H, 5.59; N, 3.10.

**Aniline salicylaldehyde Schiff-base (2).** Compound **2** was prepared through a reported procedure.<sup>13</sup>

**4-(1,2,2-triphenylvinyl)aniline-2-methoxybenzaldehyde hydrazone (3).** 2-methoxybenzaldehyde (0.20 g, 1.5 mmol) and compound **1a** (0.35 g, 1 mmol) was dissolved in 20 mL absolute ethanol in a 50 mL flask. The stirred mixture was heated to 90 °C for 2 h. Then the solvent was concentrated to 10 mL under reduced pressure and cooled to 4 °C. After that, **3** (0.35 g, 0.75 mmol) was obtained as a yellow precipitate with a yield of 75%. <sup>1</sup>H NMR (400 MHz, CDCl<sub>3</sub>),  $\delta$  (ppm): 3.92 (s, 3H), 6.97 (d, 1H), 7.12 (m, 20H), 7.46 (t, 1H), 8.16 (d, 1H), 8.94 (s, 1H). <sup>13</sup>C NMR (400 MHz, CDCl<sub>3</sub>),  $\delta$  (ppm): 55.60, 111.16, 120.66,

120.96, 126.46, 126.53, 127.57, 127.74, 127.88, 131.45, 132.23, 140.67, 140.92, 141.48, 143.89, 150.71, 155.86, 159.53. ESI-MS spectrometry:  $m/z$  calcd. for  $[M+H]^+$ : 466.2; found: 466.2. Elemental analysis, calcd. for  $C_{34}H_{27}NO$ : C, 87.71; H, 5.85; N, 3.01, found: C, 88.57; H, 5.88; N, 3.00.

### 3 Results and discussion

#### 3.1 The AIE characteristics of **1**.

The fluorescence characteristics of **1** was firstly investigated in  $H_2O/EtOH$  ( $H_2O$  is poor solvent for **1** while  $EtOH$  is good solvent for **1**, water fraction ( $f_w$ ) from 0% to 99%, v/v) buffered by 10 mmol/L PBS at pH 7.0. As shown in Figure 1, the fluorescence emission of **1** at 539 nm was rather weak in ethanol and barely increased before the  $f_w$  reached 50%. When  $f_w$  reached to 60%, the fluorescence emission suddenly enhanced, which was almost 5-fold greater than that in ethanol solution and even larger when  $f_w$  varied from 70% to 99%. The enhanced fluorescence emission could be contributed to the poor solubility of **1** in water than that in  $EtOH$ , which indicated that **1** exhibited typical AIE characteristics. The fluorescence spectra of **1** in solid state is similar to that of **1** in poor solvent ( $f_w = 99\%$ ), as can be seen in Figure 2, which further supported the AIE character.

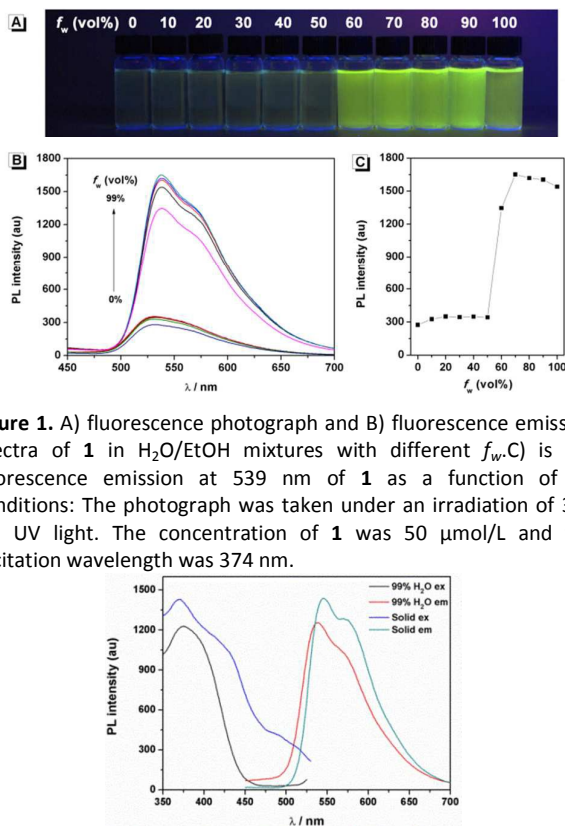


**Figure 1.** A) fluorescence photograph and B) fluorescence emission spectra of **1** in  $H_2O/EtOH$  mixtures with different  $f_w$ . C) is the fluorescence emission at 539 nm of **1** as a function of  $f_w$ . Conditions: The photograph was taken under an irradiation of 365 nm UV light. The concentration of **1** was 50  $\mu\text{mol/L}$  and the excitation wavelength was 374 nm.

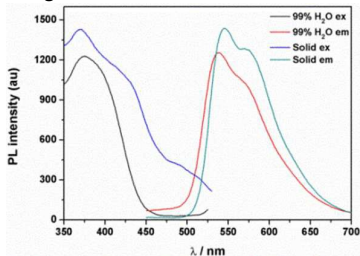


**Figure 2.** Fluorescence spectra of **1** in solid state and in poor solvent of 99%  $H_2O/EtOH$  (v/v).

To further verify that the emission enhancement was induced from aggregation, the absorption spectra of **1** in

different water fraction were measured (Figure 3B). In pure ethanol, an absorption peak of **1** at 353 nm was observed. Along with the increase of  $f_w$ , the fine structures of absorption spectra disappeared gradually, and level-off tails in the visible region could be clearly observed when  $f_w$  was higher than 50%. The level-off tails in the absorption spectra is believed to be due to the light scattering of aggregates suspensions.<sup>14</sup> The aggregation of **1** in poor solvent of water was further proved by the dynamic light scattering (DLS) measurement (Figure 3C). As shown, particles around 100 nanometer sizes were detected in aqueous solution of 99%  $H_2O/EtOH$  (v/v). On the contrary, no particle could be observed for **1** in ethanol.

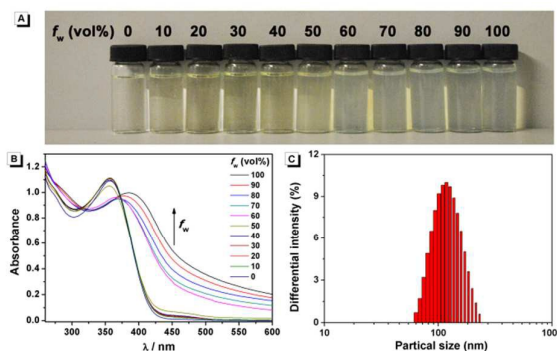


**Figure 3.** A) photograph and B) absorption spectra of **1** in  $H_2O/EtOH$  mixtures with different  $f_w$ . C) DLS result of **1** in aqueous solution of 99%  $H_2O/EtOH$  (v/v), the polydispersity index is 0.138. Conditions: The concentration of **1** is 50  $\mu\text{mol/L}$ .

#### 3.2 The origination of the AIE characteristics of **1**.

It is worth noting that the maximum fluorescence emission wavelength of **1** is remarkably longer than that of TPE monomer ( $\lambda_{max} = 453$  nm),<sup>12</sup> but similar with that of SA ( $\lambda_{max} = 542$  nm).<sup>13</sup> This result suggested that the AIE property of **1** may be not only originated from the TPE moiety but also from the salicylaldehyde hydrazone moiety. To confirm this assumption, anilinesalicylaldehyde hydrazone (**2**) and 4-(1,2,2-triphenylvinyl)aniline-2-methoxybenzaldehyde hydrazone (**3**) were chosen as control compounds. As shown in Scheme 3, compound **2** was designed in lack of the TPE part as compared to **1**. As expected, **2** exhibited no fluorescence in both  $EtOH$  and aqueous solution ( $f_w = 99\%$ ), which indicated that the TPE part in compound **1** is indispensable for its AIE property (Figure S1).

It is well known that the AIE properties for TPE and its analogues are come from the restricted intramolecular rotations (RIR) process: In good solvents, the molecules in single state and the conjugate plane of phenyl rings undergo dynamic intramolecular rotations, resulting in excited state non-radiative transition and fluorescence quenching. In poor solvents or solid state, the molecules are aggregated and the rotations are greatly restricted, which make the radiative transition to be the primary pathway for the excited state electrons back to ground state.<sup>14</sup> To further verify that the RIR process contributed to the AIE property of **1**, the fluorescence emissions of **1** in solvent with high viscosity (ethanol/glycerin)

## ARTICLE

Journal Name

were investigated. As shown in Figure 4, the fluorescence emission of **1** enhanced gradually with the increase of glycerin fraction ( $f_g$ ) because the high viscosity solvent restricted intramolecular rotations. Meanwhile, no level-off tail could be observed in their absorption spectra, which suggested there was no aggregate of **1** in glycerin. These results indicate that the RIR process is one of the main causes for the AIE property of **1**. Moreover, the RIR process is also supported by the crystal structure of **1**. Single crystal of **1** was grown from methanol/ethanol mixtures by slow solvent evaporation and was characterized by X-ray crystallography. The crystal of **1** was stable to moisture or atmosphere, and is soluble in common organic solvents such as dichloromethane, tetrahydrofuran, dimethylsulfoxide, and so on, but insoluble in water. As shown in Figure 5A, all the carbon/nitrogen atoms in the salicylaldimine moiety of **1** are in the same plane, which indicates possible intramolecular hydrogen. Meanwhile, the intermolecular distance of **1** is 5.7 Å (far over 3.8 Å<sup>15</sup>), which suggest that there is no face-to-face-stacking in the crystal (Figure 5B). All of these structural features indicated that **1** had potential of AIE properties by RIR process in aggregate state.

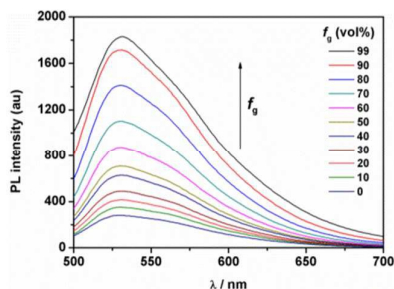


**Figure 4.** Fluorescence spectra of **1** in EtOH/glycerin mixtures with glycerin volume fraction ( $f_g$ ) from 0% to 99%. Conditions: The concentration of **1** is 50  $\mu\text{mol/L}$  and the excitation wavelength is 370 nm.

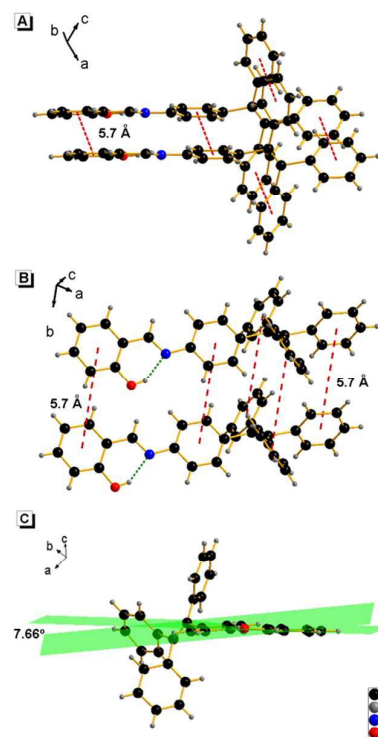


**Figure 5.** Crystal structure of **1**. A) vertical direction, B) horizontal direction, C) The dihedral angle between the two aromatic rings in N-salicylideneaniline moiety of **1**.

According to the reports, the AIE properties of SA and its analogues originated from RIR and ESIPT process: On one hand, the intramolecular hydrogen-bond in salicylaldimine moiety stabilizes the conjugated plane structure, which lead to a possible RIR process.<sup>13, 16</sup> On the other hand, a fast four-level (E-c-E\*-c-K\*-K, Figure 6) cycle occurs immediately after photo excitation of the SA molecule through the intramolecular hydrogen-bond, resulting in an ESIPT fluorescence.<sup>10a, 17</sup> Thus, when the intramolecular hydrogen-bond was broken, the AIE properties of SA and its analogues should disappear. Control compound **3** containing a methoxy group instead of the phenolic hydroxyl group was synthesized to demonstrate the role of salicylaldehyde hydrazone moiety in the AIE property of **1**. As shown in Figure S1, no fluorescence could be detected for **3** both in good and poor solvents. This result clearly demonstrated that the salicylaldehyde hydrazone moiety is indispensable for the AIE property of **1**. In addition, characteristic large Stokes shift (176 nm) could be observed in compound **1** (Figure 2), which is larger than that of the reported TPE monomer (about 60 nm<sup>12</sup>), suggesting a reasonable ESIPT process.<sup>10c, 18</sup> Therefore, ESIPT process is another main cause for the AIE effect of **1** besides the RIR process. Interestingly, compound **1** exhibits unique stability in its trans-keto form compared with conventional ESIPT molecules,<sup>17, 19</sup> which make it a potential photochromic material. The photochromic property of **1** will be further discussed in the following pages.

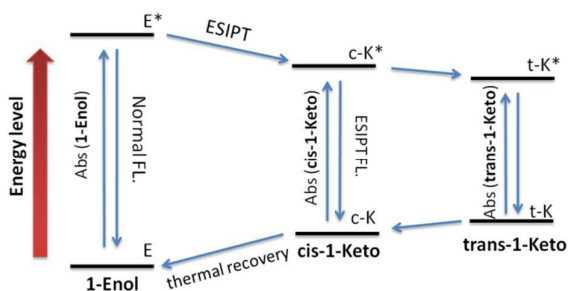


Figure 6. Four-level energy diagram of ES IPT process of **1**.

### 3.3 The reversible photochromic property of **1**.

Compound **1** was supposed to exhibit reversible photochromic property based on our design in Scheme 1, which was characterized and supported by ultraviolet-visible diffuse reflectance spectra (UV-DRS) and fluorescence spectra. As shown in Figure 7 and Video 1, **1** was yellow and there was no absorption band above 550 nm before UV light irradiation. It turned to red and exhibited a broad absorption band from 450 nm to 600 nm after UV light irradiation. When the UV light was removed, compound **1** restored to its original state gradually. In contrast, as can be seen in Figure 7B, the fluorescence emission of **1** around 545 nm was intense before UV light irradiation (fluorescence quantum yields  $\phi = 4.88\%$ ), while it decreased significantly after UV light irradiation ( $\phi = 2.03\%$ ). The fluorescence of UV-irradiated **1** also gradually recovered in dark.

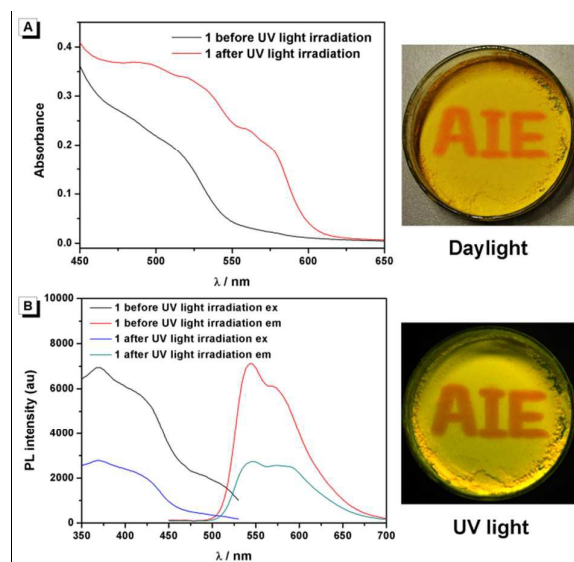


Figure 7. A) UV-DRS (left) and visible color (right) changes of **1** before and after UV light irradiation. B) Fluorescence spectra (left) and luminescence (right) changes of **1** before and after UV light irradiation. The photos in A) and B) are taken under daylight and UV light, respectively.

These photochromic properties of **1** might be attributed to the tautomerism of salicylaldehyde hydrazone from its enol-form (**1-Enol**) to trans-keto-form (**trans-1-Keto**) (Scheme 2). To

support this hypothesis, the photo-response performance of control compounds **2** and **3** were measured. As shown in Figure S2, compound **2** exhibited similar photochromic property with **1** due to its salicylaldehyde hydrazone structure: the UV light irradiation turned compound **2** from **2-Enol** into **trans-2-Keto**.<sup>9</sup> In contrast, compound **3** exhibited no photochromic property in lack of the salicylaldehyde hydrazone moiety. Therefore, it could be deduced that the salicylaldehyde hydrazone moiety of **1** was indispensable for its photochromic property.

Interestingly, compound **1** exhibits tunable thermal bleaching rate. At room temperature without light, the patterns recorded on the film of **1** can stay for hours (Figure 8). Elevated temperature would accelerate the conversion from **trans-1-Keto** back to **1-Enol** (Figure 9). The light source to promote the photochromism of **1** was investigated, which is at least in the range from 365 nm to 475 nm (Table S1). Light with longer wavelength will not promote the photochromism process but even accelerate the recovery rate. As shown in Video 1, the letters were printed in a film of **1** by a household laser point. After being irradiated by a visible light for about 10 s, the letters on the film could be erased completely. The effect of light irradiation intensity and wavelength to the recovery rate were investigated and the results were shown in Figure 10 and Table S1. The fluorescence intensity of **1** at 545 nm before and after excess UV light irradiation is 141 and 56, respectively. After keeping **1** in dark for 1 min, the intensity increased to 59. When the recovery experiments were taken under visible light of 500, 550, 600 and 650 nm (light irradiation intensity was about 2 mW/cm<sup>2</sup>), the intensity reached to 87, 110, 62 and 61, respectively. (To ensure the veracity, all of the measurements were repeated for 3 times). It can be seen that the visible light around 550 nm will accelerate the recovery rate most effectively. These results are consistent with the reported ones.<sup>20</sup>

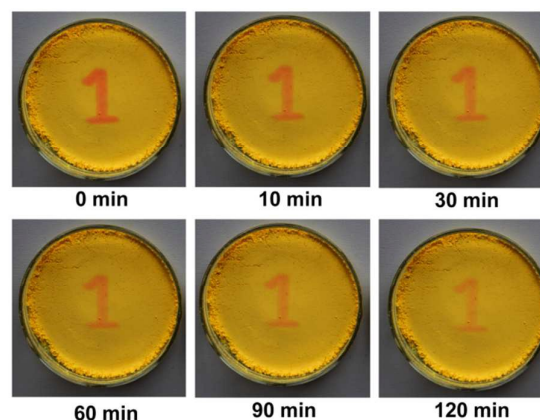


Figure 8. Photographic images of thermal bleaching of **1** in dark at room temperature.

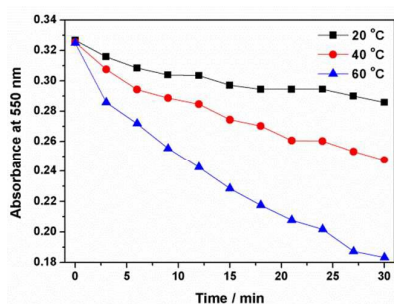


Figure 9. The thermal fading kinetics of **1** at different temperature.

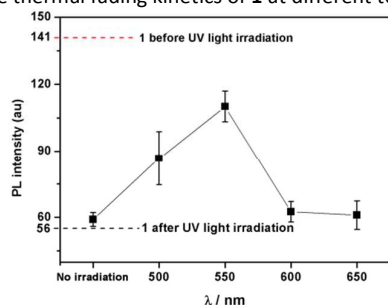


Figure 10. The dot lines are the fluorescence intensity of **1** at 545 nm before and after excess UV light irradiation. The scatterplot is the fluorescence intensity of UV-irradiated **1** at 545 nm exposed in light with different wavelength for 1 min.

According to the reports,<sup>9, 20a, 21</sup> the transformation between cis-keto form and trans-keto form is the major cause of the high stability of UV-irradiated salicylaldehyde hydrazone derivatives. To investigate the configuration of UV-irradiated **1**, the photochromic properties of **1** in different organic solvents (dispersed state) were investigated first. As shown in Figure S3, compound **1** exhibited no photochromic property in its dispersed state, which suggested that the aggregation of molecule is indispensable to the stability of UV-irradiated **1**: Since there is no steric hindrance in dispersed state, **1** is more inclined to exist as a lower energy state of cis-keto-form by thermal motion, which can easily transform to its enol-form. In aggregated state, however, the steric hindrance of contiguous molecules will limit conformational change, which is beneficial for the stability of trans-keto-form. Therefore, the UV-irradiated **1** should be trans-form in aggregation state. The trans-to-cis transformation is the rate determination step for the recovery reaction. That is why the UV-irradiated **1** can persist for hours at room temperature in dark (Figure 8).

The crystalline packing of molecules has an important effect on their optical properties. According to the reports, salicylaldehyde hydrazone can be classified into two categories, i.e., thermochromic molecules and photochromic molecules.<sup>20b, 22</sup> The thermochromic molecules were usually observed as planar structures that are closely packed in the crystal lattice. The dihedral angle between the two aromatic rings is smaller than 25°. In contrast, the photochromic molecules were usually found as twisted structures with long intermolecular distances, and the dihedral angle between the two aromatic rings is larger than 25°. Interestingly, **1** exhibited typical photochromic but not obvious thermochromic properties, although the dihedral angle between the two aromatic

rings in **1** is 7.66° (Figure 5), which is much smaller than 25°. This uncommon phenomenon can be attributed to the loose packing of the TPE moiety, which enlarged the intermolecular distance effectively. This packing is beneficial to the isomerization from cis-keto to trans-keto form under light irradiation.

It is known that the carbonyl moiety in **trans-1-Keto** is an efficient fluorescence quencher due to its strong electron-withdrawing property.<sup>11</sup> Therefore, the fluorescence intensity of **trans-1-Keto** was much weaker than that of **1-Enol**. Furthermore, the absorbance of **trans-1-Keto** at 450-600 nm is significantly higher than that of **1-Enol** (Figure 7A). Therefore, the self-absorption of **trans-1-Keto** is another reason for its weaker fluorescence intensity.

Further information about the fluorescence change of **1** was obtained from fluorescence dynamics measurement (Figure 11). The fluorescence lifetime ( $\tau$ ) of **1** before UV light irradiation is 0.83 ns, which is analogous to that of **1** after UV light irradiation (0.75 ns). Radiative decay rate constant ( $k_r$ ) and non-radiative decay rate constant ( $k_{nr}$ ) were calculated according to the definition of  $\tau = 1/(k_r + k_{nr})$  and  $\phi = k_r/(k_r + k_{nr})$ .<sup>24</sup> Before UV light irradiation,  $k_r$  and  $k_{nr}$  of **1** were  $5.88 \times 10^7 \text{ s}^{-1}$  and  $1.15 \times 10^9 \text{ s}^{-1}$ , respectively. While  $k_r$  reduced to  $2.57 \times 10^7 \text{ s}^{-1}$  and  $k_{nr}$  barely changed ( $1.23 \times 10^9 \text{ s}^{-1}$ ) after UV light irradiation. The analogous non-radiative decay process of **1-Enol** and **trans-1-Keto** suggest their similar microstructure in solid state. To confirm this assumption, X-ray powder diffractions (XRD) of **1** before and after UV light irradiation were carried out (Figure 12). It can be seen that the XRD spectra of **1** before and after UV light irradiation were almost the same, which suggest their analogous crystal structures.

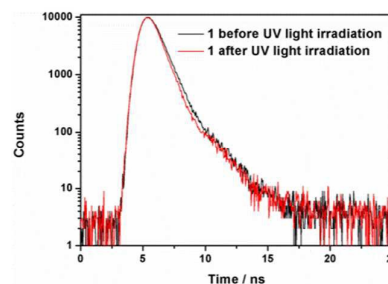


Figure 11. Comparison of fluorescence lifetimes of **1** before and after UV light irradiation.

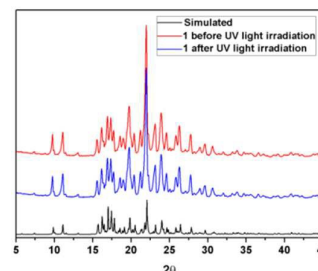
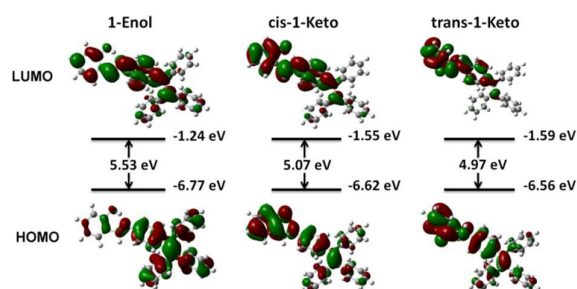


Figure 12. Comparison of XRD results of **1** before and after UV light irradiation.

To gain further insight into the photochromic properties, the calculations were performed on **1-Enol**, **cis-1-Keto** and **trans-1-**

**Keto** with Gaussian 09 program. The geometries were optimized with RM062X hybrid density function and the basis set used was 6-31+G(d,p). Theoretically, energy gap between HOMO and LUMO (EHL) is correlated with the wavelength of absorption: Smaller EHL enables the electron transit easier, resulting in a red-shift of absorption wavelength.<sup>25</sup> As shown in Figure 13, the EHL of **1-Enol** is 5.53 eV and the EHL of **trans-1-Keto** is 4.97 eV. These calculated results agree well with the red-shifted absorption wavelength obtained by experiments (Figure 7A). Meanwhile, compared with **1-Enol**, the HOMO and LUMO of **cis-1-Keto** and **trans-1-Keto** distributed mainly in the area near to the carbonyl moiety, which visually demonstrated the electron-withdrawing property of carbonyl moiety. In addition, the total energy (sum of electronic and zero-point energies) of **cis-1-Keto** and **trans-1-Keto** was calculated to be -38137.6774 eV and -38137.2176 eV, respectively. The higher total energy of **trans-1-Keto** indicates that the trans-form is a metastable form of UV-irradiated **1**. **1** is more inclined to exist as a lower energy state of **cis-1-keto** in dispersed state, which can easily transform to its **1-Enol**. Thus, the photochromic property is difficult to be observed in dispersed state. Meanwhile, the total energy of **cis-1-Keto** and **trans-1-Keto** are both higher than that of **1-Enol** (-38137.9985eV), suggesting that the compound have gained energy from UV light after irradiation.



**Figure 13.** Frontier molecular orbital amplitude plots and energy levels of the HOMOs and the LUMOs of **1-Enol**, **cis-1-Keto** and **trans-1-Keto**. Value of contour envelopes is 0.02 au.

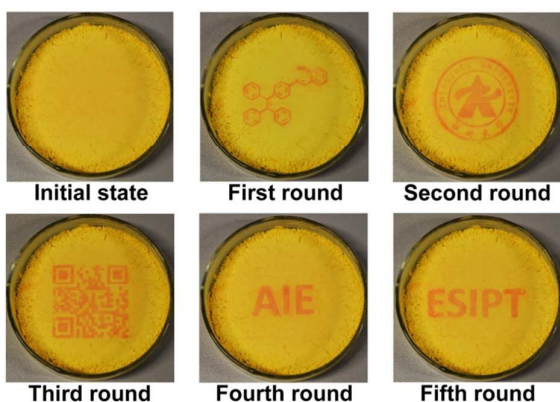


**Figure 14.** Generating different patterns on the same film of **1**.

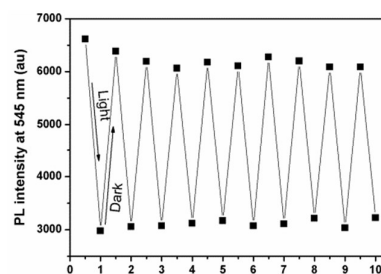


**Figure 15.** Fatigue resistance of **1** upon UV light irradiation and standing in dark alternatively.

As a reversible photochromic material, **1** was capable of serving as a material for photo-patterning with erasable property. As shown in Figure 14, letters, 2-dimensional bar code and other patterns could be recorded on the same film of **1**. The process was rather simple as discussed below. Pre-organized pattern was firstly printed in transparencies, then UV light was allowed to pass through it onto the film of **1** and the pattern was subsequently recorded. Other patterns could be recorded on the same film after the former pattern disappeared gradually in dark or was erased quickly by long wavelength light irradiation. The fatigue resistance of **1** was investigated by toggled repeatedly between **1-Enol** and **trans-1-Keto** for 10 times. As shown in Figure 15, the fluorescence at 545 nm stayed almost constant without degradation, indicating a good fatigue resistance of **1**. The reversible, controllable photochromic properties, as well as the good fatigue resistance of **1** indicate that it can be served as promising solid material for erasable photo-patterning.

In conclusion, a specially designed AIE molecule of **1** connecting TPE and SA moieties has been developed. Compound **1** exhibits typical AIE properties due to RIR and ESIPT process. Compare with TPE monomer, compound **1** has longer fluorescence emission wavelength of 545 nm and larger Stokes shift of 176 nm. As a photochromic molecule, compound **1** shows reversible color and fluorescence changes upon UV light irradiation. More importantly, recovery rate from **trans-1-Keto** back to **1-Enol** is controllable by temperature and long wavelength light irradiation. **1** also shows good fatigue resistance, which makes it an excellent candidate for photo-patterning with erasable property. Compared with the conventional caged photo-activatable system, photo-induced redox system and photo-induced cyclization system, this work provides a brand new strategy in the design of reversible photo-controllable luminescent system.

## Acknowledgements

This research was supported by the National Natural Science Foundation of China (No.21501150, 51502079, 21371155) and Outstanding Young Talent Research Fund of Zhengzhou University (1521316005). We are grateful for the helpful advices in our experiments from Benzhong Tang's lab of HKUST.

## Notes and references

1. a) S. M. Borisov and O. S. Wolfbeis, *Chem. Rev.*, 2008, **108**, 423; b) Z. Chi, X. Zhang, B. Xu, X. Zhou, C. Ma, Y. Zhang, S. Liu and J. Xu, *Chem. Soc. Rev.*, 2012, **41**, 3878; c) L. Ying, C. L. Ho, H. Wu, Y. Cao and W. Y. Wong, *Adv. Mater.*, 2014, **26**, 2459; d) Y. Tao, K. Yuan, T. Chen, P. Xu, H. Li, R. Chen, C. Zheng, L. Zhang and W. Huang, *Adv. Mater.*, 2014, **26**, 7930.
2. R. Hu, N. N. L. Leung and B. Z. Tang, *Chem. Soc. Rev.*, 2014, **43**, 4494.
3. J. Luo, Z. Xie, J. W. Y. Lam, L. Cheng, H. Chen, C. Qiu, H. S. Kwok, X. Zhan, Y. Liu, D. Zhu and B. Z. Tang, *Chem. Commun.*, 2001, 1740.
4. a) D. Ding, K. Li, B. Liu and B. Z. Tang, *Acc. Chem. Res.*, 2013, **46**, 2441; b) R. Hu, L. Nelson L C and B. Z. Tang, *Chem. Soc. Rev.*, 2014, **43**, 4494; c) Z. Zhao, B. He and B. Z. Tang, *Chem. Sci.*, 2015, **6**, 5347.
5. C. Y. Y. Yu, R. T. K. Kwok, J. Mei, Y. Hong, S. Chen, J. W. Y. Lam and B. Z. Tang, *Chem. Commun.*, 2014, **50**, 8134.
6. L. Peng, Y. Zheng, X. Wang, A. Tong and Y. Xiang, *Chem.-Eur. J.*, 2015, **21**, 4326.
7. a) T. Kobayashi, T. Komatsu, M. Kamiya, C. Campos, M. Gonzalez-Gaitan, T. Terai, K. Hanaoka, T. Nagano and Y. Urano, *J. Am. Chem. Soc.*, 2012, **134**, 11153; b) A. Rodrigues Correia, W. Xenia M M and A. Heckel, *Org. Lett.*, 2013, **15**, 5500.
8. a) X. Gu, E. Zhao, J. W. Y. Lam, Q. Peng, Y. Xie, Y. Zhang, K. S. Wong, S. H. H. Y., I. D. Williams and B. Z. Tang, *Adv. Mater.*, 2015, **27**, 7093; b) D. Ou, T. Yu, Z. Yang, T. Luan, Z. Mao, Y. Zhang, S. Liu, J. Xu, Z. Chi and M. R. Bryce, *Chem. Sci.*, 2016, **7**, 5302; c) X. Gu, E. Zhao, T. Zhao, M. Kang, C. Gui, J. W. Y. Lam, S. Du, M. M. T. Loy and B. Z. Tang, *Adv. Mater.*, 2016, **28**, 5064.
9. E. Hadjoudis and I. M. Mavridis, *Chem. Soc. Rev.*, 2004, **33**, 579.
10. a) M. Sliwa, N. Mouton, C. Ruckebusch, S. p. Aloïse, O. Poizat, G. Buntinx, R. Métivier, K. Nakatani, H. Masuhara and T. Asahi, *J. Phys. Chem. C*, 2009, **113**, 11959; b) J. Zhao, S. Ji, Y. Chen, H. Guo and P. Yang, *Phys. Chem. Chem. Phys.*, 2012, **14**, 8803; c) V. S. Padalkar and S. Shu, *Chem. Soc. Rev.*, 2015, **45**, 169; d) L. McDonald, J. Wang, N. Alexander, H. Li, T. Liu and Y. Pang, *J. Phys. Chem. B*, 2016, **120**, 766.
11. N. E. Schore and N. J. Turro, *J. Am. Chem. Soc.*, 1975, **97**, 2482.
12. H. Yuan, K. Wang, K. Yang, B. Liu and B. Zou, *J. Phys. Chem. Lett.*, 2014, **5**, 2968.
13. W. Tang, Y. Xiang and A. Tong, *J. Org. Chem.*, 2009, **74**, 2163.
14. a) J. Chen, C. C. W. Law, J. W. Y. Lam, Y. Dong, S. M. F. Lo, I. D. Williams, D. Zhu and B. Z. Tang, *Chem. Mater.*, 2003, **15**, 1535; b) A. Qin, J. W. Y. Lam, F. Mahtab, C. K. W. Jim, L. Tang, J. Sun, H. H. Y. Sung, I. D. Williams and B. Z. Tang, *Appl. Phys. Lett.*, 2009, **94**, 253308; c) J. Shi, N. Chang, C. Li, J. Mei, C. Deng, X. Luo, Z. Liu, Z. Bo, Y. Q. Dong and B. Z. Tang, *Chem. Commun.*, 2012, **48**, 10675; d) J. Mei, Y. Hong, J. W. Y. Lam, A. Qin, Y. Tang and B. Z. Tang, *Adv. Mater.*, 2014, **26**, 5429.
15. C. Janiak, *J. Chem. Soc., Dalton Trans.*, 2000, 3885.
16. Q. Feng, Y. Li, L. Wang, C. Li, J. Wang, Y. Liu, K. Li and H. Hou, *Chem. Commun.*, 2016, **52**, 3123.
17. M. Ziółek, J. Kubicki, A. Maciejewski, R. Naskręcki and A. Grabowska, *Phys. Chem. Chem. Phys.*, 2004, **6**, 4682.
18. J. Zhao, S. Ji, Y. Chen, H. Guo and P. Yang, *Phys. Chem. Chem. Phys.*, 2011, **14**, 8803.
19. M. Ziółek, J. Kubicki, A. Maciejewski, R. Naskręcki and A. Grabowska, *Chem. Phys. Lett.*, 2003, **369**, 80.
20. a) H. Koshima, K. Takechi, H. Uchimoto, M. Shiro and D. Hashizume, *Chem. Commun.*, 2011, **47**, 11423; b) F. Robert, P. L. Jacquemin, B. Tinant and Y. Garcia, *Crystengcomm*, 2012, **14**, 4396.
21. F. Robert, A. D. Naik, F. Hidara, B. Tinant, R. Robiette, J. Wouters and Y. Garcia, *Eur. J. Org. Chem.*, 2010, **4**, 621.
22. a) K. Ogawa, Y. Kasahara, Y. Ohtani and J. Harada, *J. Am. Chem. Soc.*, 1998, **120**, 7107; b) X. T. Chen, Y. Xiang, P. S. Song, R. R. Wei, Z. J. Zhou, K. Li and A. J. Tong, *J. Lumin.*, 2011, **131**, 1453; c) M. Avadanei, V. Cozan, S. Shova and J. A. Paixão, *Chem. Phys.*, 2014, **444**, 43.
23. a) F. Robert, A. D. Naik, B. Tinant, R. Robiette and Y. Garcia, *Chem.-Eur. J.*, 2009, **15**, 4327; b) F. Robert, A. D. Naik, F. Hidara, B. Tinant, R. Robiette, J. Wouters and Y. Garcia, *Eur. J. Org. Chem.*, 2010, **4**, 621.
24. Z. Chang, L. Jing, C. Wei, Y. Dong, Y. Ye, Y. Zhao and J. Wang, *Chem. - Eur. J.*, 2015, **21**, 8504.
25. a) B. Li, J. Wang, H. Wen, L. Shi and Z. Chen, *J. Am. Chem. Soc.*, 2012, **134**, 16059; b) F. Hu, M. Cao, X. Ma, S. Liu and J. Yin, *J. Org. Chem.*, 2015, **80**, 7830; c) C. T. Poon, W. H. Lam, H. L. Wong and V. W. Yam, *Chem.-Eur. J.*, 2015, **21**, 2182.

Aggregation-induced emission (AIE) molecule with reversible photochromic property which can be served as a material for photo-patterning with erasable property

